

Transcriptome Dynamics of Developing Photoreceptors in Three-Dimensional Retina Cultures Recapitulates Temporal Sequence of Human Cone and Rod Differentiation Revealing Cell Surface Markers and Gene Networks

ROSSUKON KAEWKHAW,^{a,b} KORAY DOGAN KAYA,^a MATTHEW BROOKS,^a KOHEI HOMMA,^{a,e} JIZHONG ZOU,^{c,d} VIJENDER CHAITANKAR,^a MAHENDRA RAO,^{c,f} ANAND SWAROOP^a

Key Words. Human rod and cone photoreceptors • Stem cells • Global gene profiling • Next generation sequencing • Three-dimensional organoid culture • Retina

ABSTRACT

The derivation of three-dimensional (3D) stratified neural retina from pluripotent stem cells has permitted investigations of human photoreceptors. We have generated a H9 human embryonic stem cell subclone that carries a green fluorescent protein (GFP) reporter under the control of the promoter of cone-rod homeobox (*CRX*), an established marker of postmitotic photoreceptor precursors. The *CRX*_p-GFP reporter replicates endogenous *CRX* expression in vitro when the H9 subclone is induced to form self-organizing 3D retina-like tissue. At day 37, *CRX*⁺ photoreceptors appear in the basal or middle part of neural retina and migrate to apical side by day 67. Temporal and spatial patterns of retinal cell type markers recapitulate the predicted sequence of development. Cone gene expression is concomitant with *CRX*, whereas rod differentiation factor neural retina leucine zipper protein (*NRL*) is first observed at day 67. At day 90, robust expression of *NRL* and its target nuclear receptor *NR2E3* is evident in many *CRX*⁺ cells, while minimal S-opsin and no rhodopsin or L/M-opsin is present. The transcriptome profile, by RNA-seq, of developing human photoreceptors is remarkably concordant with mRNA and immunohistochemistry data available for human fetal retina although many targets of *CRX*, including phototransduction genes, exhibit a significant delay in expression. We report on temporal changes in gene signatures, including expression of cell surface markers and transcription factors; these expression changes should assist in isolation of photoreceptors at distinct stages of differentiation and in delineating coexpression networks. Our studies establish the first global expression database of developing human photoreceptors, providing a reference map for functional studies in retinal cultures. *STEM CELLS* 2015;33:3504–3518

SIGNIFICANCE STATEMENT

We describe the development of a new human embryonic stem cell reporter line that faithfully recapitulates endogenous protein expression during retinal development. Using this reporter hESC line, we have established an organoid 3-dimensional culture system that should serve as a model for investigating human photoreceptor development in vitro. We have purified developing human photoreceptors from organoid cultures and produced global gene expression profiles using next generation sequencing. Our transcriptome analysis provides a reference data set to delineate gene regulatory networks underlying human photoreceptor differentiation and to elucidate how mutations in retinopathy genes affect cell fate, maturation and/or homeostasis. We expect that the cell line, the data sets and the protocols we have developed will be of immense value to the scientific community.

INTRODUCTION

In humans, vision is arguably the most important of all senses with more than 30% of the brain dedicated to the analysis of visual information. The visual process begins in the retina

where photons are captured by two kinds of photoreceptors—rods and cones, having distinct morphology, unique visual pigment(s), and specialized functions. Photoreceptors constitute 75%–80% of cells in the human retina, with rods being 95% of all photoreceptors [1];

^aNeurobiology-Neurodegeneration & Repair Laboratory, National Eye Institute, National Institutes of Health, Bethesda, Maryland, USA; and ^bResearch Center, Faculty of Medicine Ramathibodi Hospital, Mahidol University, Bangkok, Thailand; ^cCenter for Regenerative Medicine, National Institutes of Health, Bethesda, Maryland, USA; ^diPSC Core, Center for Molecular Medicine, National Heart, Lung, and Blood Institute, Bethesda, Maryland, USA; ^eDepartment of Physiology, Nippon Medical School, Tokyo, Japan; ^fThe New York Stem Cell Foundation Research Institute, New York, NY 10023

Correspondence: Anand Swaroop, Ph.D., Neurobiology-Neurodegeneration & Repair Laboratory, National Eye Institute, National Institutes of Health, Bldg 6/338, 6 Center Drive, MSC 0610, Bethesda, Maryland 20892, USA. Telephone: 301-435-5754; Fax: 301-480-9917; e-mail: swaroop@nei.nih.gov

Received April 8, 2015; accepted for publication June 28, 2015; first published online in *STEM CELLS EXPRESS* July 31, 2015.

This article was published online on 14 August 2015. An error was subsequently identified. This notice is included in the online and print versions to indicate that both have been corrected 4 September 2015.

© AlphaMed Press
1066-5099/2014/\$30.00/0

<http://dx.doi.org/10.1002/stem.2122>

This is an open access article under the terms of the Creative Commons Attribution-NonCommercial License, which permits use, distribution and reproduction in any medium, provided the original work is properly cited and is not used for commercial purposes.

however, unlike most mammals (including rodents), the human retina has a unique spatial organization of rods and cone subtypes with higher relative density of cones in central retina (called macula) and a rod-free zone in the fovea [1, 2]. Differential and/or regional dysfunction or death of photoreceptors in the human retina leads to impairment of peripheral or central vision in retinal and macular degenerative diseases [3, 4], a major cause of incurable blindness worldwide. Mutations or variations in almost 250 genes have been associated with retinal diseases (www.sph.uth.tmc.edu/Retnet/), representing unprecedented phenotypic and genetic heterogeneity and a challenge for clinical management and therapy. Elucidation of pathways underlying human photoreceptor development should facilitate the design of novel treatment paradigms for blinding retinal diseases.

Our current understanding of photoreceptor differentiation is primarily based on studies in mice and other model organisms [5–8]. Six major types of retinal neurons and Muller glia are generated from distinct pools of retinal progenitor cells that pass through unique competence states capable of producing one or more cell types under the guidance of an intrinsic genetic program. A large number of transcription factors, including OTX2, thyroid hormone receptor b2 ($TR\beta 2$), cone-rod homeobox (CRX), neural retina leucine zipper protein (NRL), and NR2E3, control photoreceptor development [6]. Of these, CRX is the first gene specifically detected in all postmitotic photoreceptor precursors [9] and is critical for regulating the expression of both cone and rod genes [10, 11]. NRL and $TR\beta 2$ determine rod and M-cone fate, respectively. Loss of NRL produces S-cones instead of rods in mouse retina [12], whereas S-cones are generated instead of M-cones in the absence of $TR\beta 2$ [13]. Furthermore, ectopic expression of NRL and $TR\beta 2$ produces rods and M-cones, respectively [14, 15]. Thus, S-cones appear to be the default fate of mammalian photoreceptor precursors [6, 15].

Anatomical and immunohistochemical studies using human fetal retina show similarities as well as distinct characteristics [16]. CRX is detected as early as fetal week (Fwk) 9–10, whereas expression of NRL and NR2E3 follows at Fwk 10.5–11 [17]. Opsin expression is observed late—S-opsin at Fwk 11, rhodopsin and L/M opsin by Fwk 14–16, whereas other cone and rod proteins are detected between Fwk 11 and 18 [16]. While the photoreceptors across the retina exhibit mature morphology by Fwk 34, the fovea is still immature at birth with late maturation of foveal cones and continued rod genesis postnatally in the peripheral retina [16]. The human retina seems to be fully mature morphologically by 5 years. Understandably, molecular insights into human retinal and photoreceptor development have been lacking.

Pluripotent stem cell-derived differentiated cells can serve as a comprehensive model [18, 19] for investigating cell fate and organogenesis [20]. Human embryonic stem cells (hESCs) and induced pluripotent stem cells (hiPSCs) have been successfully used to generate rod and cone photoreceptors [21–24]. More recently, self-organizing neural retina-like tissue has been produced in three-dimensional (3D) cultures from human pluripotent stem cells [25–28]. These 3D organoids contain distinct retinal cell types and exhibit stratification of neuronal layers, making it possible to investigate human retina development and disease in vitro.

Here, we report the generation of a CRXp-green fluorescent protein (GFP) reporter hESC (H9) line to identify photoreceptor precursors at birth (i.e., at final mitosis) and following their differentiation in 3D neural retina (NR) cultures. We have used this system for live cell sorting and defined the temporal transcriptome dynamics during the establishment of cone and rod photoreceptor fate. Our studies provide an essential framework for delineating molecules and cellular pathways that guide human photoreceptor development and should assist in chemical screening and cell-based therapies of retinal degeneration.

MATERIALS AND METHODS

Human ESC Culture

H9 hESCs were maintained in feeder-free condition according to WiCell method (www.wicell.org). Cells were cultured in mTeSR1 medium (Stem Cell Technologies, Vancouver, Canada; www.stemcell.com) on BD Matrigel-hESC-qualified Matrix-coated plates with medium changed every day. Details are described in Supporting Information.

Reporter hESC Line Generation

The CRX promoter sequence [29] was cloned (–2,310 to +1) from bacterial artificial chromosome using forward primer 5'GTTAGGGGCCAGGCTGAGTG 3' and reverse primer 5'GGGGGACTCGACTGGGCA'. The promoter was ligated with GFP and subcloned into donor plasmids (pZDonor-AAVS1, Sigma-Aldrich, St. Louis, MO; <http://www.sigmaaldrich.com>), which were electroporated into mouse retina to test promoter function [30]. The strategy for gene targeting is illustrated in Figure 1A. CRX promoter construct was integrated into safe harbor AAVS1 locus by zinc finger nuclease (CompoZr Targeted Integration Kits, Sigma-Aldrich, St. Louis, MO; <http://www.sigmaaldrich.com>). Details of generating the reporter hESC line are described in Supporting Information.

Human ESC Differentiation into 3D Neural Retina

The differentiation was performed as described [25], with the following modifications. Human ESCs were dissociated by Accu-max (Stem Cell Technologies, Vancouver, Canada; www.stemcell.com) containing 10 μ M Y-27632. Basal differentiation medium contained GMEM, 20% (vol/vol) knockout serum replacement, 0.1 mM nonessential amino acids, 1 mM pyruvate, 100 U/ml penicillin, and 100 mg/ml streptomycin (Sigma-Aldrich, St. Louis, MO; www.sigmaaldrich.com). Cells on day 0 were quickly aggregated in low attachment 96-well-plates with V-bottom shape (NOF corporation, Tokyo, Japan; www.nof.co.jp/english/business/life/contact.html) (9,000 cells per well in 100 μ l) containing basal differentiation medium plus 3 μ M IWR-1-endo (Wnt inhibitor, Calbiochem, Billerica, MA; www.emdmillipore.com) and 20 μ M Y-27632. Matrigel (growth factor reduced, BD Biosciences, San Jose, CA; www.bdbiosciences.com) solution (10 μ l of 1.8 μ g/ μ l) was added in day 2 cultures. Aggregates were maintained for 4 days when half of the medium was changed with medium containing 3 μ M IWR-1-endo and Matrigel (180 μ g/ml). At day 12, aggregates were transferred to low attachment 90 mm Dishes (NOF Corporation, Tokyo, Japan; www.nof.co.jp/english/business/life/contact.html) containing basal differentiation medium, 10% (vol/vol) fetal bovine serum (FBS) (Atlanta Biological, Norcross, GA; Biological,

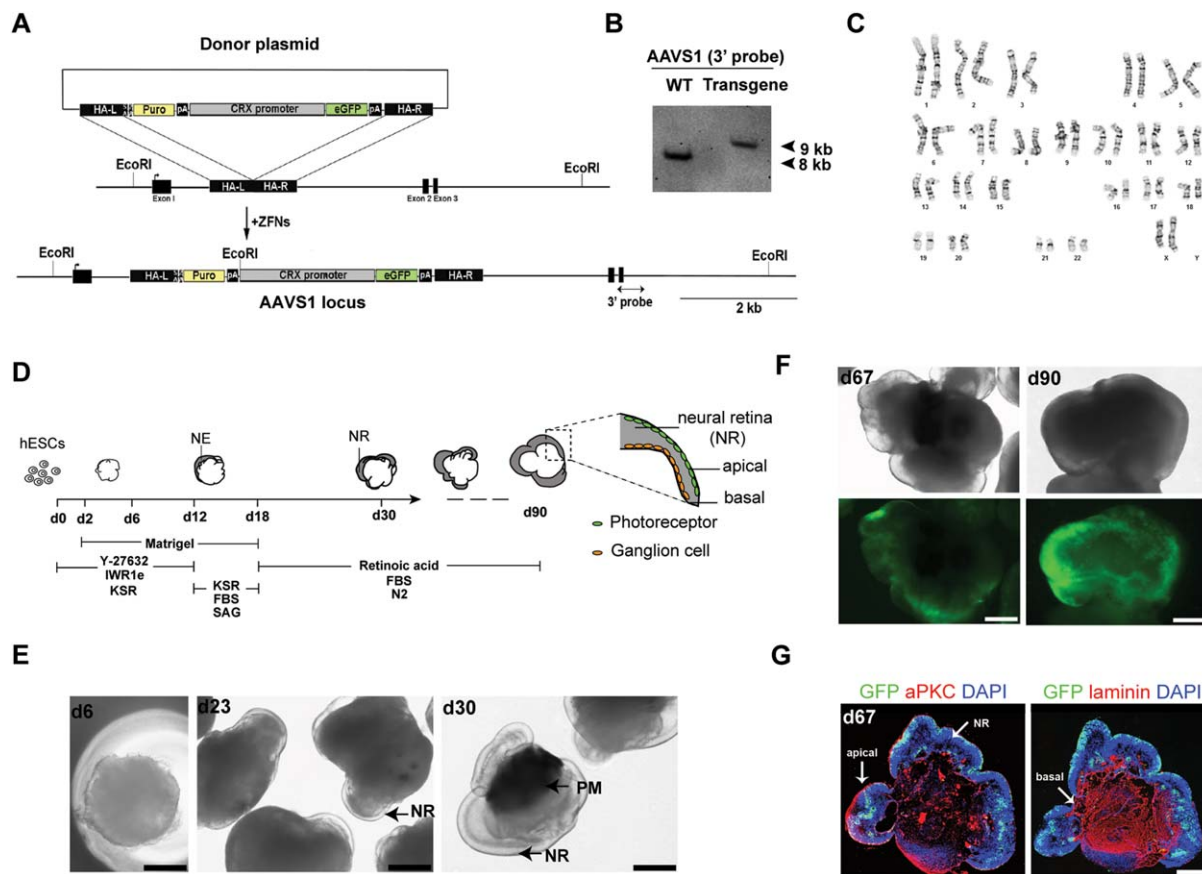


Figure 1. Generation of *CRXp*-GFP H9 hESC line and its differentiation to NR in 3D organoid cultures. **(A):** Schematic diagram illustrates transgene insertion. A functional *CRX* promoter driving GFP (Supporting Information Fig. S1A) is inserted into *AAVS1* locus of H9-hESC lines. **(B):** Validation of transgene insertion by Southern blot analysis. **(C):** Karyotype analysis of *CRXp*-GFP H9 hESC line. Staining of pluripotent marker proteins is shown in Supporting Information Figure S1B. **(D):** Schematic diagram illustrates differentiation protocol and the formation of NE and NR in aggregates. High magnification of NR indicates polarity and used to refer for Figures 2–4. IWR1e: Wnt inhibitor; SAG: hedgehog activator. **(E):** Development and expansion of a multilayered NR derived from NE, while pigmented mass (PM) is present in aggregates. PM may represent retinal pigment epithelium (RPE) or ciliary pigmented cells that are formed in aggregates derived from human pluripotent stem cells when retinal differentiation is induced [31, 32]. **(F):** GFP expression in NR generated from *CRXp*-GFP hESCs. Refer also Supporting Information Fig. S1C–S1F. **(G):** Immunostaining indicates establishment of NR polarity. aPKC and laminin staining point out apical and basal NR, respectively. DAPI-stained nucleus. Scale bar = 500 μ m (E: day 23 and day 30, F and G); 200 μ m (C: day 6). Abbreviations: 2A, 2A peptide; FBS, fetal bovine serum; HA-L and HA-R, homologous arm left and right; hESCs, human embryonic stem cells; KSR, knockout serum replacement; NE, neuroepithelium; NR, neural retina; SA, splice acceptor; ZENs, zinc-finger nucleases.

Norcross, GA; www.atlantabio.com) and 100 nM Smoothed Agonist (Hedgehog agonist, Enzo Life Sciences, Farmingdale, NY; www.enzolifesciences.com/). On day 18, the medium was switched to maintenance medium (Dulbecco's modified Eagle's medium [DMEM]/F-12 containing 1% N2 supplement [Invitrogen, Grand Island, NY; www.lifetechnologies.com/us/en/home.html], 10% [vol/vol] FBS, 0.5 μ M retinoic acid [Sigma-Aldrich, St. Louis, MO; www.sigmaaldrich.com], 0.25 mg/ml Fungizone [GIBCO, Grand Island, NY; www.lifetechnologies.com/us/en/home/brands/gibco.html], 100 U/ml penicillin, and 100 mg/ml streptomycin). Human ESC-NR were grown in maintenance medium in bacterial-grade Dishes from day 18 onwards at 40% O₂ and 5% CO₂, and the medium was changed every 3 days.

Immunohistochemistry and Live Imaging

Human ESC-NR were fixed using 3.7% formaldehyde, washed twice with phosphate-buffered saline, and incubated in 30% (wt/vol) sucrose overnight before embedding in OCT compound. Cryosections (10–12 μ m) were mounted on slides for

immunostaining, live imaging, and antibodies, as described in Supporting Information.

Fluorescence-Activated Cell Sort

3D NR cultures were collected at day 37, day 47, day 67, and day 90 and dissociated into single cells by incubating in 1:1 Accumax/TryPLE solution at 37°C for 60 minutes, with 10 times-pipetting every 20 minutes. Cell suspension was centrifuged at 4°C, 400g for 5 minutes, and cell pellets were resuspended in sorting buffer (HEPES containing 1 mM EDTA, 2.5 mM HEPES, pH 7, 1% [wt/vol] bovine serum albumin). Cells were sorted at 4°C by FACSaria (Becton Dickinson, Hunt Valley, MD; www.bd.com). GFP⁺ and GFP⁻ cells were separately collected in collecting buffer (DMEM:F-12 plus 50% [vol/vol] FBS). FSC-H and FSC-W and SSC-H and SSC-W were examined for all cells to obtain live single GFP⁺ cells. 3D NR derived from hESCs without the transgene were used to determine gate for sorting. Total RNA was extracted by RNA purification kit (Norgen Biotek, Thorold, Canada;

norgenbiotek.com) and analyzed by 2100 Bioanalyzer (Agilent Technologies Genomics, Santa Clara, CA; www.genomics.agilent.com/en/home.jsp).

RNA-seq and Data Analysis

High quality total RNA (40–60 ng, RIN: 7.7–9.2) was subjected to directional RNA-seq library construction from three independent biological replicates at each culture stage. Sequencing was performed as described [33, 34] using GALLx (Illumina, Inc., San Diego, CA; www.illumina.com) [35]. FASTQ files were generated from reads passing Chastity filter and analyzed for differential expression, cluster, and network analyses, as detailed in Supporting Information. Recombinant DNA procedures, described here, followed NIH guidelines. RNA-seq data have been deposited in Gene Expression Omnibus and are accessible through accession number GSE67645 (www.ncbi.nlm.nih.gov/geo/query/acc.cgi?acc=GSE67645).

RESULTS

Generation of CRXp-GFP H9 Line

Taking advantage of a reported mouse *Crx* promoter [29], we identified a corresponding conserved human *CRX* promoter region that was used to tag new-born (postmitotic) photoreceptors with GFP reporter (Fig. 1A). The human *CRXp*-GFP construct demonstrated development and cell type-specific GFP expression in neonatal mouse retina (Supporting Information Fig. S1A). The validated construct was targeted to AAVS1 “safe harbor” locus in hESC line, H9 (Fig. 1A, 1B). *CRXp*-GFP H9 cells retained normal karyotype and expressed relevant pluripotent markers (Fig. 1C, Supporting Information Fig. S1B).

3D Retina from CRXp-GFP H9 Cells

The *CRXp*-GFP H9 line was induced to produce NR using a previously reported 3D differentiation protocol [25], except that whole cell aggregates were maintained in culture without further manipulations permitting better reproducibility under our conditions. Fully compacted aggregates were observed within day 4 and day 6 of culture (Fig. 1D, 1E). A transparent neuroepithelium could be identified at or after day 6 and was clearly evident by day 10 (Fig. 1D, 1E). Multicell layered optic structures were observed by day 23 with NR expanding with culture time, while a pigmented mass appeared at the center of aggregates (Fig. 1D, 1E). GFP+ cells were identified as early as day 30 (Supporting Information Fig. S1C–S1E), and their number increased with culture time (Fig. 1F, Supporting Information Fig. S1F). *CRXp*-GFP+ cells were 4.0% ± 0.8%, 9.0% ± 2.9%, 15.0% ± 4.7%, and 15.1% ± 3.0% (mean ± SD, $n = 3$; >1,000 cells for each) at days 37, 47, 67, and 90, respectively. The efficiency of NR induction from *CRXp*-GFP H9 cells was 60%–80% as revealed by GFP expression. NR exhibited polarity as indicated by atypical protein kinase C and laminin staining (Fig. 1G). NR facing the cell-free cavity filled with basement membrane (i.e., laminin) was identified as the basal side, while apical side of NR was toward the culture medium (Fig. 1D, 1G). We conclude that 3D organoid culture recapitulates major aspects of retinal biology and can be used to assess photoreceptor development mediated by CRX.

Characteristics of CRX+ Photoreceptor Precursors in 3D Neural Retina

We first assessed whether GFP+ cells were indeed postmitotic, as has been reported in mice [9]. Phosphohistone-H3 and Ki67 staining revealed a proliferative zone (PZ; Ki67+ and pH3+) and a nonproliferative zone (NPZ; Ki67– and pH3–) in apical and basal NR, respectively (Fig. 2A). Ki67+ dividing cells exhibited variable labeling and occupied most of the NR at day 37, whereas pH3+ cells (in mitosis) were present at the apical surface. GFP+ cells were detected in PZ and NPZ, but none was positive for pH3 or Ki67 (Fig. 2A). At day 90, pH3+ cells in NR continue to reside at the apical surface but begin to segregate from CRX+ postmitotic photoreceptors. During early mouse retinal development, immature photoreceptors were observed with dividing progenitors in outer neuroblastic layer (ONBL), while new-born neurons resided in inner neuroblastic layer (INBL) [36, 37]. Therefore, PZ and NPZ detected in early 3D retina cultures likely represent ONBL and INBL, respectively.

The location of GFP+ cells in NR was altered during development from day 37 to day 90 (Fig. 2B, 2C). We observed two distinct zones—most GFP+ cells resided in the basal-most region at day 37 and occupied both apical and basal NR at day 47, but these cells were present apically by day 67 and day 90 (Fig. 2B, 2C). PAX6 and SIX3, two key eye-field transcription factors, are required for neuronal differentiation in the retina [38–40]. PAX6 was distributed in a gradient, where differentially labeled cells were identified in NR at all culture stages. Most cells with strong PAX6 labeling were located in NPZ whereas weakly stained cells were in PZ (Fig. 2A, 2B), consistent with their reported expression in differentiating or dividing mouse retinal progenitors, respectively. GFP+ cells were not labeled with PAX6, although some cells in NPZ of day 37 and day 47 NR expressed PAX6 (Fig. 2A, 2B). Similarly, SIX3+ cells with variable labeling were detected in NR at all stages. Except few cells residing in NPZ at day 37 and day 47, none of the GFP+ cells was positive for SIX3 (Fig. 2A, 2C). Live-cell imaging of day 42–day 44 retina demonstrated slow migration of GFP+ cells from basal to apical surface (Fig. 2D, 2E, Supporting Information Movie S1). Thus, GFP+ cells are postmitotic and represent the migration of photoreceptors to the apical side during early stages of differentiation in the 3D retina.

Differentiation of Neurons and Muller Glia in 3D Neural Retina

To examine whether 3D NR derived from *CRXp*-GFP H9 cells recapitulated in vivo development, we performed immunohistochemistry using antibodies against cell-type and lineage-specific proteins. Cone arrestin (ARR3) expression was observed first at day 47 only in few GFP+ cells which resided in the apical-most NR, and the number of ARR3+/GFP+ cells increased at later stages (Fig. 3A). Recoverin (RCVRN), a pan-photoreceptor marker, was detected in GFP+ cells at all stages from day 37 to day 90 (Fig. 3B). The presence of ganglion, horizontal, and amacrine cells was demonstrated by immunostaining with BRN3B (a ganglion cell transcription factor), Calbindin (CALB1), and Calretinin (CALB2) (markers for interneurons) (Fig. 3C, 3D). In general, ganglion cells and interneurons were located at the basal side (NPZ) of NR. Protein kinase C- α , which identifies ON bipolar cells, was

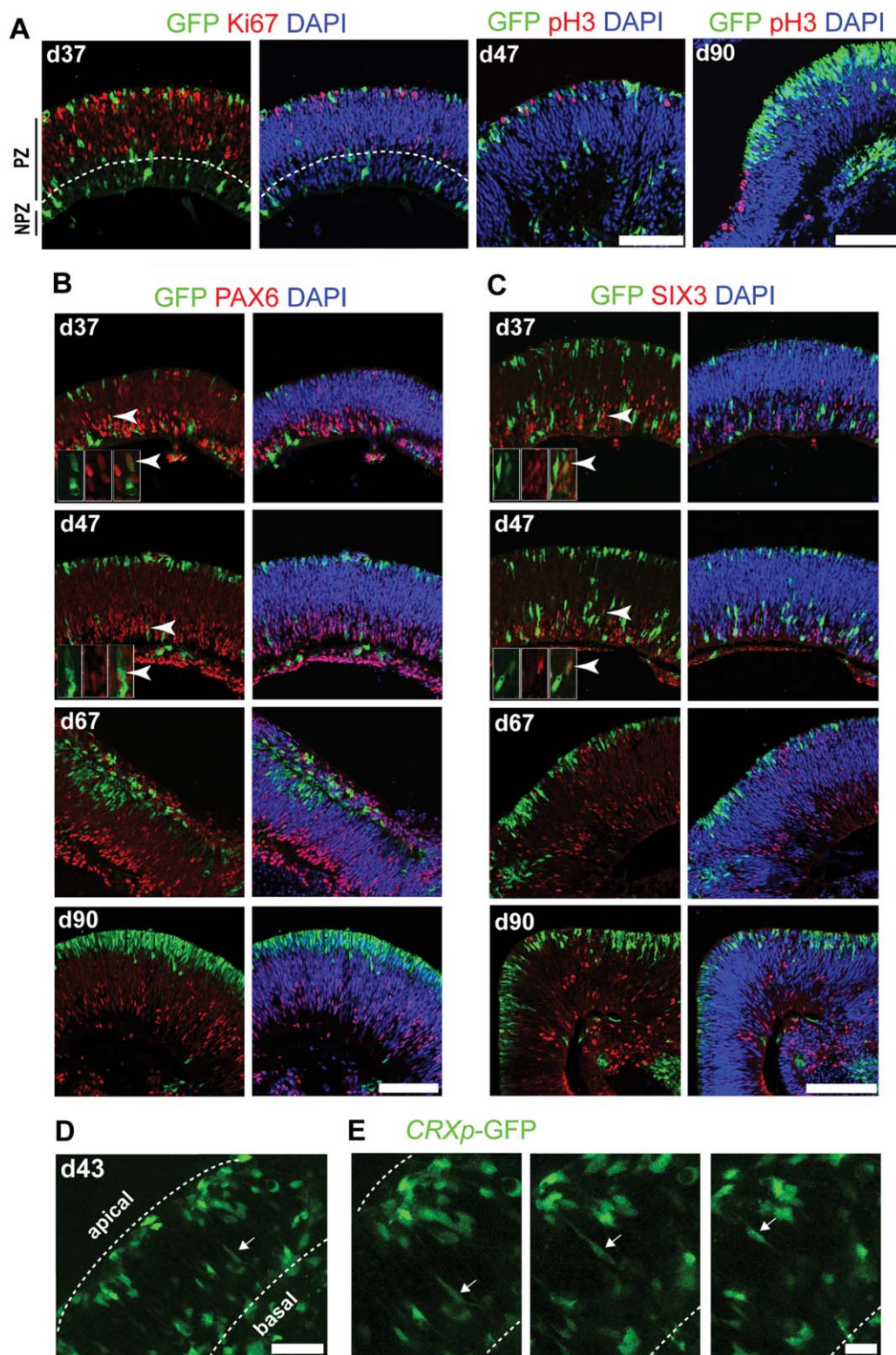


Figure 2. Characteristics of postmitotic *CRXp*-GFP+ cells in 3D neural retina. **(A):** Immunostaining for proliferative markers Ki67 and phospho-histone H3 (pH3). **(B, C):** Immunostaining for PAX6 (B) or SIX3 (C) in PZ and NPZ. Arrowhead and inserted figure indicate colocalization in few GFP+ cells. **(D, E):** Time-lapse images show migration of *CRXp*-GFP+ cells toward apical side. High magnification of a *CRXp*-GFP+ cell (arrow) (E) in D. Refer Supporting Information Movie S1. DAPI-stained nucleus. Scale bar = 100 μ m (A–C); 50 μ m (D); and 20 μ m (E). Abbreviations: GFP, green fluorescent protein; NPZ, nonproliferative zone; PZ, proliferative zone.

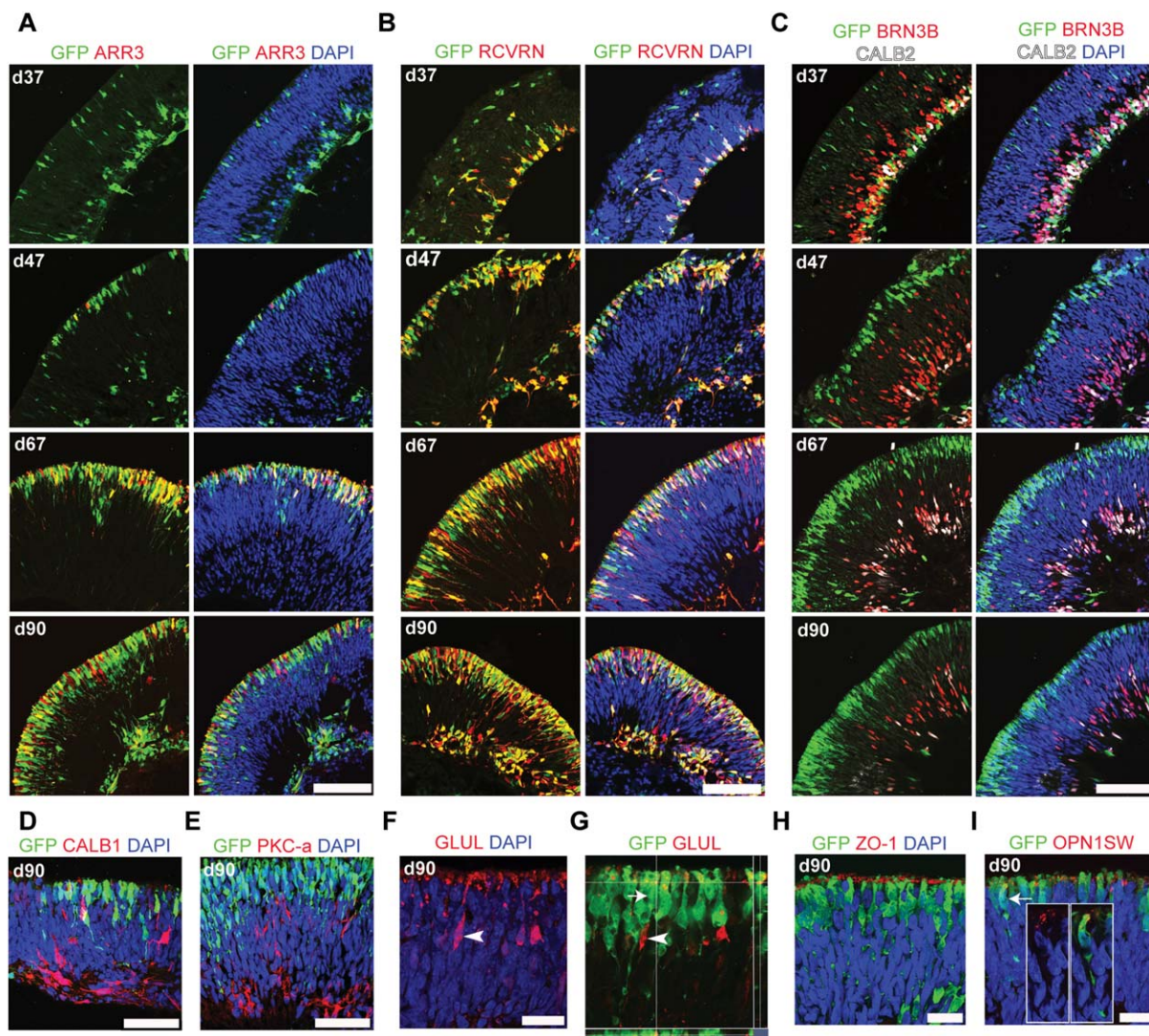


Figure 3. Expression of photoreceptor and nonphotoreceptor proteins in 3D neural retina. **(A, B):** Immunostaining for photoreceptor proteins. ARR3 (A) and RCVRN (B). **(C–G):** Immunostaining for nonphotoreceptor proteins. BRN3B (C) for ganglion cells, CALB2 and CALB1 for horizontal and amacrine cells (C and D), PKC-alpha for bipolar cells (E), or GLUL for Müller glia cells (arrow head) (F and G), which exhibit close contact with photoreceptors (arrow) (G). **(H):** Immunostaining for tight junction ZO-1. **(I):** Immunostaining for opsin expression. Arrow head points the GFP+ cell for high magnification. Refer also Supporting Information Figure S2A–S2D. DAPI-stained nucleus. Scale bar = 100 μm (A–C); 50 μm (D–E); 20 μm (F–H). Abbreviation: GFP, green fluorescent protein.

detected in few cells at day 90 basally to CRX+ photoreceptors (Fig. 3E). Müller glia cells, labeled by Glutamine Synthetase (GLUL), were observed only in day 90 NR (Fig. 3F, 3G); these cells extended processes toward outer limiting membrane-like structure (ZO1 staining), establishing close contact with GFP+ cells (Fig. 3F–3H). We conclude that, as predicted, CRX+ GFP expressing cells are immature postmitotic precursors, which begin differentiation into photoreceptors at day 67 in 3D cultures.

While minimum S-opsin (OPN1SW) immunostaining was detected in a punctate pattern at day 90 (Fig. 3I), S-opsin was appropriately localized to the plasma membrane and in segment-like structures at day 126 and day 180 (Supporting Information Fig. S2A, S2B). Rod and L/M cone visual pigments (RHO and L/M-opsin, respectively) were not detected at day 90 but were present in the plasma membrane as segment-like structures when NR was maintained for 150 days or longer (Supporting Infor-

mation Fig. S2C, S2D show data at day 180). GFP+ cells generally formed a rosette-like structure after day 90 in the region of opsin-expressing cells, as reported recently [28] (Supporting Information Fig. S2B–S2D). These rosette-like structures contain photoreceptors with their apical side located at the center of the rosette. In the same retinal organoid, the photoreceptors can remain well organized at the apical surface even at a late stage (day 160 or day 180) yet may also appear in the middle or basal side as rosette-like structures. Many such structures can be maintained up to day 200 in retinal organoids. The photoreceptors in rosettes and at the apical surface of neural retina appear to be produced by independent processes in 3D cultures.

Development of Photoreceptors in 3D Neural Retina

We evaluated expression pattern of key transcription factors associated with photoreceptor development in GFP+ cells

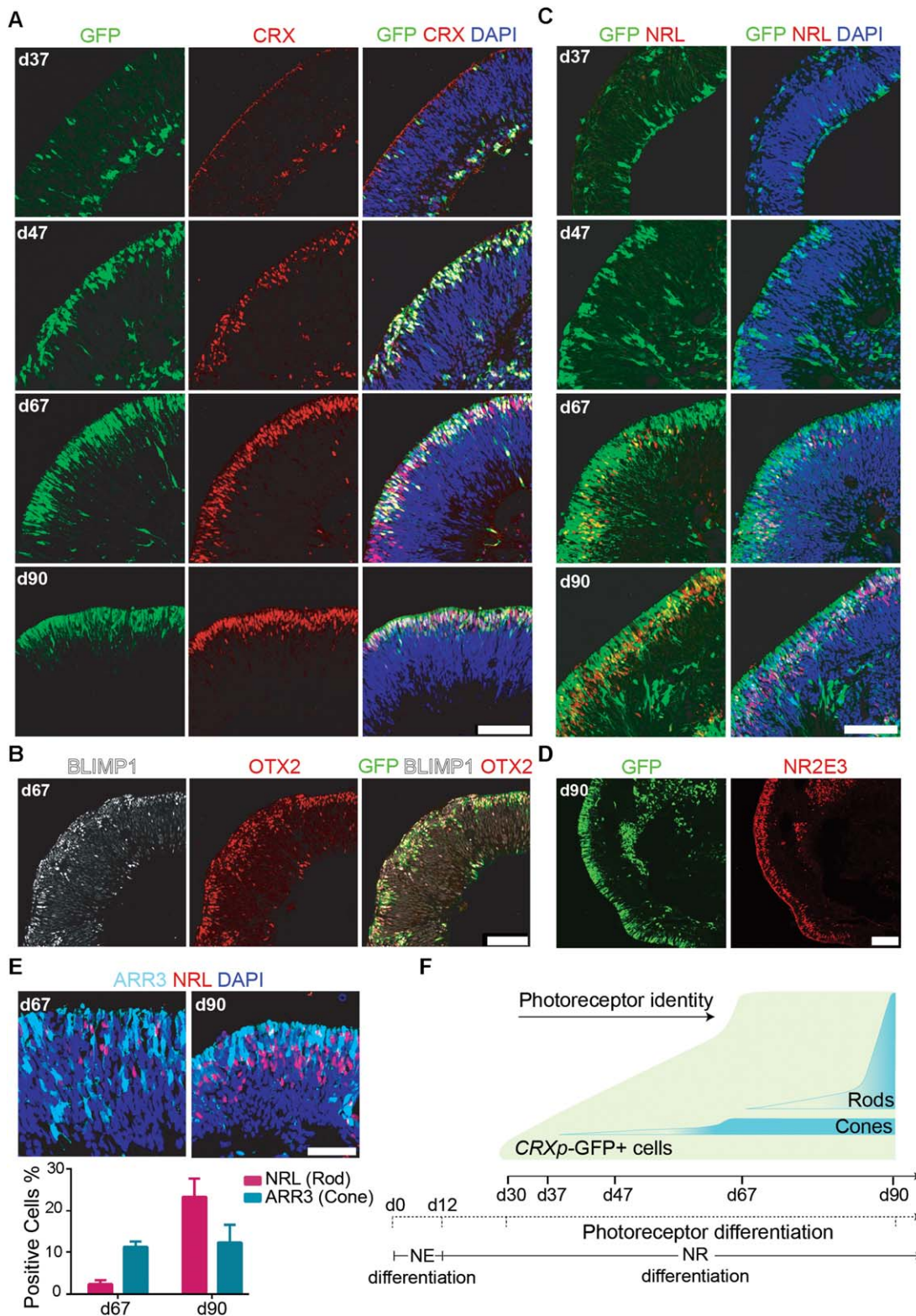


Figure 4. Expression patterns of lineage-specific proteins determining photoreceptor fates. **(A–D)**: Immunostaining for transcription factors: CRX (A), BLIMP1 and OTX2 (B), NRL (C), and NR2E3 (D). Refer also in Supporting Information Figure S2E–S2G. The background signal of CRX observed on the apical side at day 37 is distinguishable from the immunostaining within the cells at the basal side. **(E)**: Coimmunostaining of NRL (rod) and ARR3 (cone). Percentage of cells (DAPI-stained nuclei) that are immunostained with NRL and ARR3 is shown as mean \pm SD, $n = 3$ independent experiments. **(F)**: Schematic diagram representing lineage progression of CRX ρ -GFP photoreceptors. DAPI staining identifies nucleus. Scale bar = 100 μ m (A–D); 50 μ m (E). Abbreviations: GFP, green fluorescent protein; NE, neuroepithelium; NR, neural retina.

(Fig. 4). CRX was detectable in almost 90% of GFP+ developing photoreceptors at all stages examined (day 37, $91.3\% \pm 2.1\%$; day 47, $92.5\% \pm 7.3\%$; day 67, $86.9\% \pm 8.3\%$; day 90, $91.4\% \pm 5.4\%$; mean \pm SD, $n = 3$) (Fig. 4A). Endogenous CRX is expressed under the control of native regulatory elements, and the *CRXp*-GFP construct introduced at the AAVS1 site may not completely replicate the expression efficiency. All GFP+ cells also expressed OTX2 (Supporting Information Fig. S2E), which initiates expression of CRX [41], and BLIMP1 that restricts bipolar cell competence biasing them toward photoreceptor fate [42] (Fig. 4B). Noticeably, not all OTX2+ or BLIMP1+ cells were positive for GFP (Fig. 4B). OTX2 and CRX regulate the expression of NRL [33, 43, 44], which determines rod photoreceptor cell fate and in turn controls the expression of NR2E3 [45]. NRL or NR2E3 expression was not evident until day 67 when GFP+ cells occupied the apical-most NR (Fig. 4C, Supporting Information Fig. S2F). NRL and NR2E3-positive cells increased at day 90 and thereafter (Fig. 4C, 4D; Supporting Information Fig. S2G). We conclude that rod fate is acquired at a later stage of development in CRX+ photoreceptors.

We then identified developing cones and rods by costaining with ARR3 and NRL, respectively, in 3D NR cultures (Fig. 4E). While the number of ARR3+ cones was constant ($11.4\% \pm 1.3\%$ to $12.4\% \pm 4.2\%$) from day 67 to day 90, NRL+ developing rods increased by almost 10-fold ($2.4\% \pm 0.9\%$ to $23.3\% \pm 4.4\%$) during this period (Fig. 4E). Thus, the expanded temporal window of photoreceptor differentiation in human retina seems to be reflected in H9 hESC-derived 3D neural retina and nicely separates the birth of cones and rods (Fig. 4F).

Transcriptome of Developing Human Photoreceptors

With a goal to elucidate molecular signatures associated with distinct stages of human photoreceptor development, we performed transcriptome analyses of three independent sets of flow-sorted GFP+ cells at each time point using RNA-seq (Fig. 5). Cells from 3D neural retina were obtained at the same stage to exclude autofluorescence (Fig. 5A). The enrichment of photoreceptors in the sorted population is evident by difference in CRX expression between GFP+ and GFP- cells (Fig. 5B), and quality control metrics demonstrated high degree of correlation and reproducibility (Fig. 5B, 5C).

Lineage- or cell-type-specific gene expression was used to verify the state of differentiation (Fig. 5D, Supporting Information Fig. S3A, S3B). Pluripotency markers were detected only in undifferentiated H9 cells, and expression of pan-neuronal markers demonstrated differentiation into neuronal rather than glial or neural crest lineage of sorted GFP+ cells (Supporting Information Fig. S3A). Synaptophysin, which is expressed in cone photoreceptors, was detected in GFP+ photoreceptors while Synapsin I [17] was absent. The expression of DCX, a marker of migrating neurons, was initially high in GFP+ cells but was much lower at day 90 (Supporting Information Fig. S3A). Several retinal transcription factors (PAX6, LHX2, VSX2, ATOH7, and NEUROD4), but not the RPE factor Microphthalmia-associated Transcription Factor, were expressed at high levels initially and, as predicted, their expression was lower by day 67 and day 90 (Supporting Information Fig. S3A). OLIG2 and NEUROG2 were undetectable by day 90 (Supporting Information Fig. S3A). The tran-

scripts for several transcription factors, including OTX2, RAX, SIX3, SIX6, and ASCL1, were unchanged or higher as cone and rod cell fates were established (Supporting Information Fig. S3A).

Transcription regulatory factors and their target genes associated with structure and function of retinal ganglion cells and interneurons (such as POU4F2, FOXN4, PTF1A, and ONECUT1) [46–49] were detectable initially at day 37 and day 47 in GFP+ cells, but these genes were not expressed by day 90 (Supporting Information Fig. S3B). Genes enriched in retinal progenitors and Müller glial cells [50, 51] were detectable but at very low levels (HES1, HES5, ID1, and ID3) in GFP+ cells at day 67 and day 90 (Supporting Information Fig. S3B). However, we noticed high expression of few bipolar (LHX3, VSX1, GRM6, and CABP5) and Müller glial (DBI, GNAI2, GLUL, and DKK3) enriched genes in GFP+ cells of 3D retina at all culture stages examined (Supporting Information Fig. S3B), suggesting developmental plasticity.

Several photoreceptor-specific genes exhibited a gradual and continuous increase in expression with time. In general, cone genes showed high expression before rod-specific genes, further validating the genesis of cones before rods (Fig. 5D). Rod-specific genes (such as NR2E3, NRL, GNAT1, and CNGB1) were upregulated at day 90, yet the late stage transcriptional regulators, including estrogen-related receptor beta (ESRRB) and myocyte-specific enhancer factor 2C (MEF2C) (detected by postnatal days 7 and 33 in mouse retina, respectively [52, 53]) and transcripts for phototransduction proteins were undetectable in GFP+ cells (Fig. 5D). Although we observed some immunostaining for S-opsin at day 90, RNA-seq data did not show significant S-opsin transcripts. The transcriptome profile thus indicates an immature photoreceptor state of GFP+ cells even as late as day 90 in these cultures of H9 hESC-derived 3D NR.

When compared with day 37 GFP+ cells (newborn photoreceptors), the number of genes that showed more than or equal to twofold increase at day 47, day 67, or day 90 (in developing cones and rods) were 265, 1,422, and 1,942, respectively (Fig. 5E). The proteasome complex genes, PSMA6 and PSMC6, were enriched at day 47, with concurrent downregulation of cell cycle-associated genes, CSNK1D and CDK7. High expression of Prominin-1 (PROM1 or CD133), potassium channel KCNV2, and Complexin 4 at day 67 and day 90 demonstrated acquisition of photoreceptor specialization by GFP+ cells (Fig. 5E). NRL expression was enriched at day 90, supporting rod-dominance in 3D NR at this stage (Fig. 5E).

The top 10 highly expressed transcription factors included RAX2 and RXRG, which were present at all time points compared with day 37 (Supporting Information Fig. S3C). POU4F2, ONECUT3, ID1, FOSB, E2F5, AEBP1, MORF4L1, and DBX1 were enriched at day 37 in at least two pairwise comparisons. SMARCE1 and PRMT1 were enriched at day 47 and day 67, while DMBX1 was expressed high at day 67 and day 90 (Supporting Information Fig. S3C). NRL and NR2E3 were highly expressed at day 90 (Supporting Information Fig. S3C). Our results confirm that GFP expressing postmitotic cells lose markers of dividing progenitors and other retinal cell types as they undergo differentiation to cone and rod fate sequentially over a prolonged period of time in the human 3D retina.

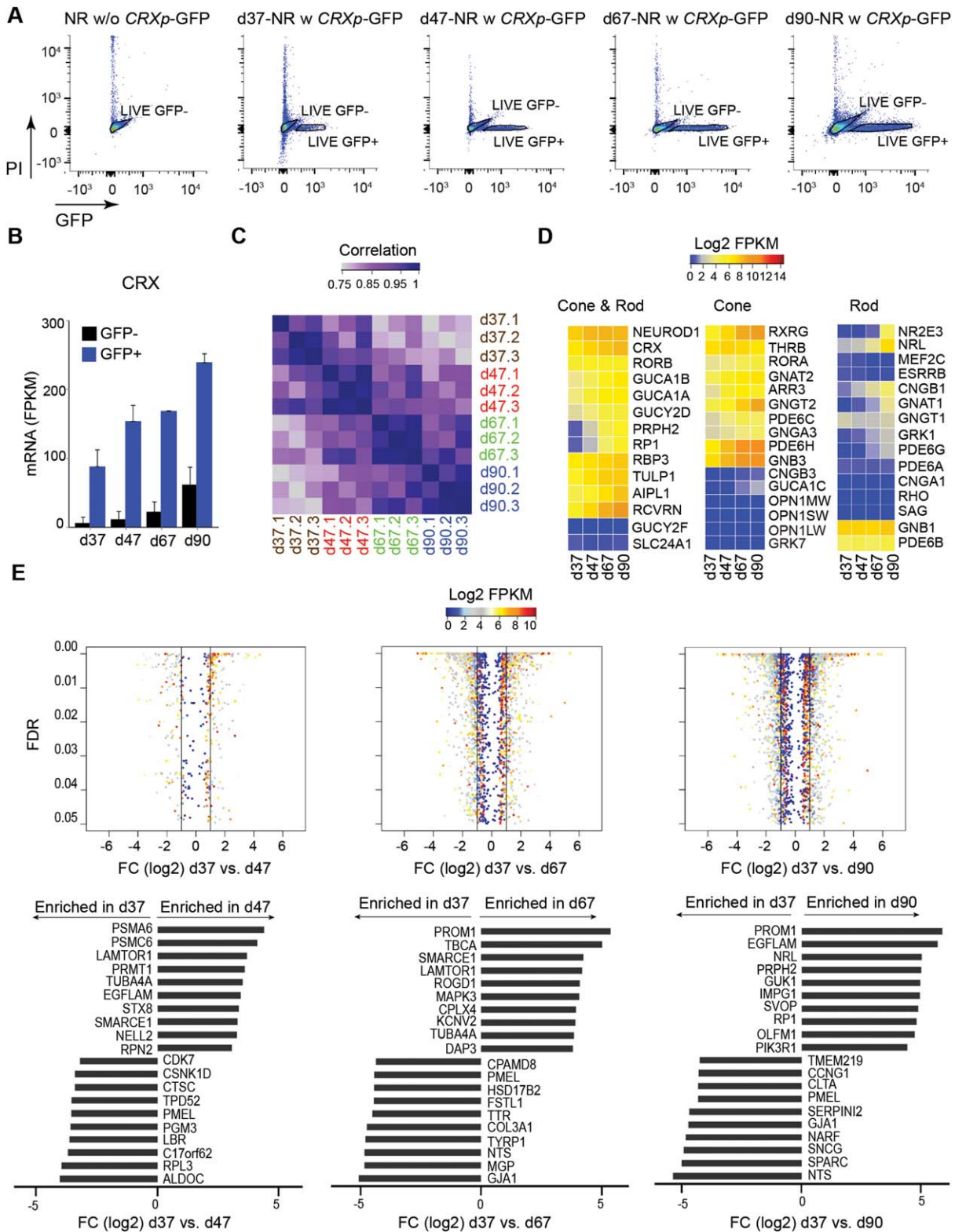


Figure 5. Enrichment and expression analysis of *CRXp*-GFP⁺ cells. **(A):** Dot plots indicate flow-sorted GFP⁺ cells. Human embryonic stem cells with *CRXp*-GFP (not shown) and aggregates without *CRXp*-GFP at the same culture stage with sample are used as a negative control. **(B):** Bar graph shows CRX expression in GFP-positive and negative fractions. Data are shown as mean FPKM \pm SD from RNA-seq data, $n = 3$ independent experiments for GFP⁺ cells, two independent experiments for GFP⁻ cells. **(C):** Clustering of biological replicates. Heat map of RNA-seq data represents similarity of sorted samples from blue (highest) to light purple (smallest). **(D):** Heat map represents expression of cone and rod-associated genes in flow-sorted GFP⁺ cells. Refer also Supporting Information Figure S3A, S3B for nonphotoreceptor lineage-associated genes. **(E):** Volcano plots indicate fold change in expression. Top 10 differentially expressed genes are shown from comparisons between day 37 versus day 47, day 37 versus day 67, and day 37 versus day 90. For transcription factor genes, refer also Supporting Information Figure S3C. Abbreviations: GFP, green fluorescent protein; NR, neural retina.

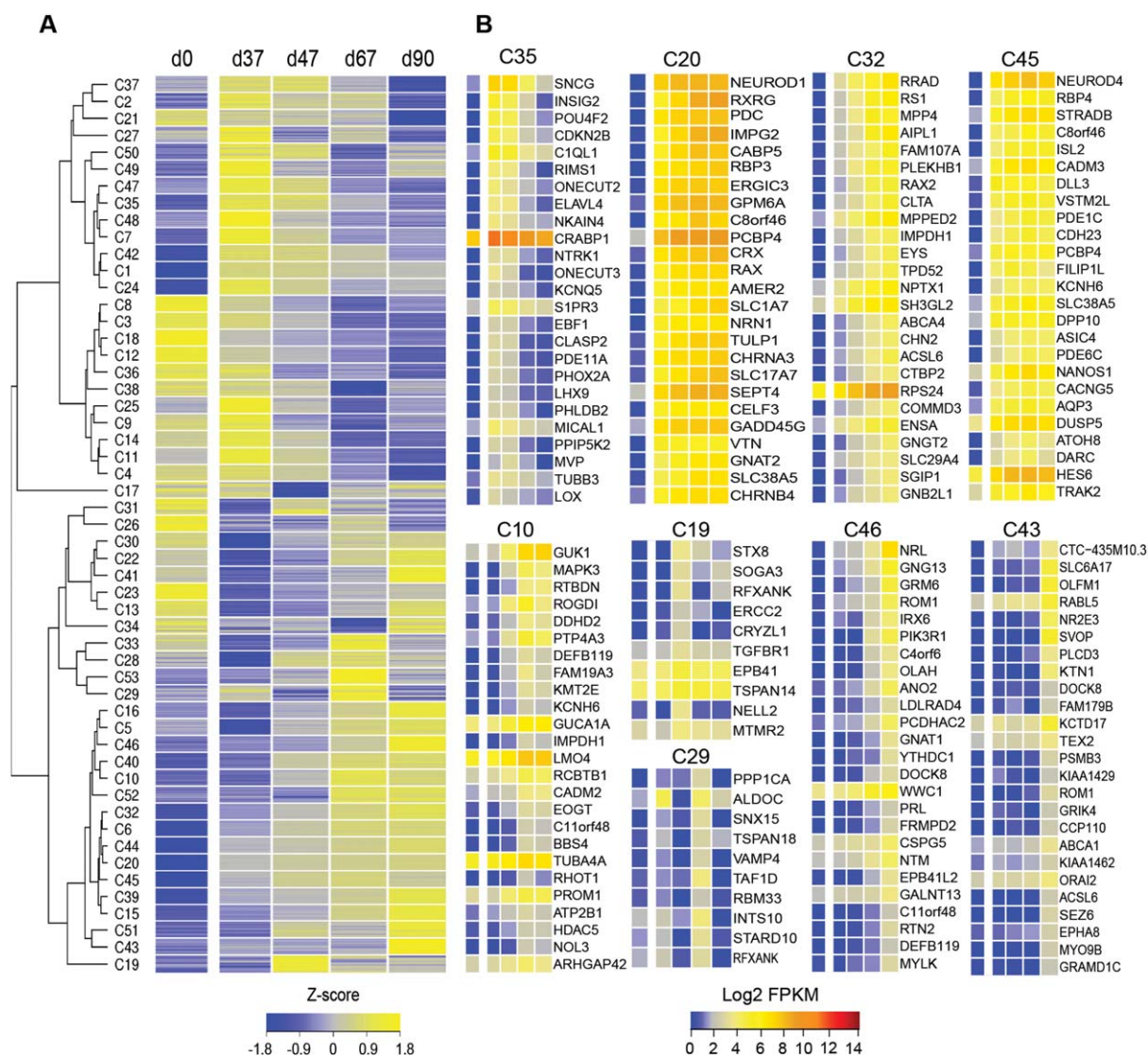


Figure 6. Cluster analysis of differentially expressed genes. **(A):** Heat map represents gene expression pattern in each cluster. Refer Supporting Information Figure S4A, S4B for gene ontology analysis. Transcripts of cell surface molecules are extracted from each cluster, as shown in Supporting Information Figure S6. **(B):** Heat maps indicate top 25 (or all genes if <25) highly expressed genes in clusters of retina-expressed genes or clusters with unique expression at specific stages (see C19 and C29). Refer also Supporting Information Figure S5A–S5D.

Cluster Analysis of Gene Expression Patterns in Developing Photoreceptors

Immunostaining and transcriptome analysis suggested a window between day 47 and day 67 for cone development, whereas rod differentiation began at day 67 with the expression of NRL. The patterns of 3,157 transcripts revealed developmentally dynamic expression, and differentially expressed transcripts formed 53 distinct clusters (C) (Fig. 6A, Supporting Information Fig. S4A). Gene ontology (GO) analysis ($p < .05$) revealed significant enrichment of neuronal differentiation, eye development, and visual perception biological processes in several clusters (Supporting Information Fig. S4B), while positive regulators of cell cycle progression were in clusters 12 and 18; the latter were highly expressed in hESCs and downregulated upon differentiation (Supporting Information Fig. S4A, S4B). The genes associated with vascular development were enriched in clusters 3, 9, 14, and 49 and showed

decreased expression at later stages in CRX+ photoreceptors (Supporting Information Fig. S4A, S4B).

We then focused on clusters of eye-field and/or retina-expressed genes that revealed unique expression patterns at distinct time points. Expression of genes in C1, C7, C24, C35, C42, and C47 clusters was high in day 37 GFP+ cells and decreased with time (Fig. 6A, 6B, Supporting Information Fig. S5A); these genes indicated retinal lineage transition and genetic footprint of progenitors. Cyclin-dependent kinase inhibitors (CDKNIA, p21 (C24)), a negative regulators of G1 cell cycle progression, and multiple transcription factors expressed in early-born retinal neurons (PAX6, ATHO7, NR2F1, NR2F2, PRDM1, and ONECUT proteins) also belonged to these clusters (C1, C24 and C35 and C42) (Fig. 6B, Supporting Information Fig. S5A). Thyroid hormone receptor beta (C1) associated with M-cone differentiation in mouse retina exhibited peak expression at day 47 (Supporting Information Fig. S5A), concordant with its peak expression in E17 developing mouse

retina followed by decline at later stages [54]. Similarly, genes in C19, including STX8, NELL2, and ERCC2, showed specific expression at day 47 (Fig. 6B). Their function has not been reported during photoreceptor development.

The genes in C6, C20, and C44 were highly expressed in photoreceptors in addition to CRX, and these include OTX2, NEUROD1, CPLX4, GUCA1B, RCVRN, and AIPL1 (Fig. 6B, Supporting Information Fig. S5B). The photoreceptor genes in C32, C40, and C52 (such as PROM1, RAX2, ABCA4, RS1, and RPGRIP1) revealed a similar pattern but had lower expression initially at day 37 and/or day 47 (Fig. 6B, Supporting Information Fig. S5B). Furthermore, cone-specific genes including GNAT2, GNB3, RXRG, ARR3, GNGT2, and CNGA3 were readily identifiable in these clusters.

The genes with high expression at day 67 were present in C10 and C45, where CHRN4 and PDE6C were identified as cone-specific genes (Fig. 6B). Several transcription regulatory proteins (NEUROD4, ISL2, ATOH8, HES6, LMO4, KMT2E, and HDAC5) may be selectively associated with cone differentiation as they are coexpressed with cone-specific genes in these clusters (Fig. 6B). GUK1 and GUCA1A, although expressed in both photoreceptor subtypes, are also part of these clusters (Fig. 6B). The genes in C29, C33, and C53 were unique in that their expression was specific at day 67 (Fig. 6B, Supporting Information Fig. S5C). High level of transcripts at day 90 in C15, C16, C39, C43, and C46 demonstrated coexpression with rod-specific genes that include NRL, NR2E3, and GNAT1 (Fig. 6A, 6B, Supporting Information Fig. S5D). Other photoreceptor-expressed genes, such as Netrin-G2, Cadherin (CDHR1), ROM1, and CNGB1 are also present in these clusters, suggesting further maturation by day 90.

Potential Cell Surface Markers at Distinct Stages of Photoreceptor Development

Previous studies suggested the requirement of committed yet immature developing photoreceptors for replacement therapy in mouse retina [55]. To facilitate the isolation of human developing photoreceptors, we extracted potential transmembrane and cell surface molecules from clusters, using EBI's QuickGO. The present dataset was compared with the published transcriptomes of rods (*Nrl*-GFP/wt) and cone-like cells (*Nrl*-GFP/*Nrl*^{-/-}) [56] (Supporting Information Fig. S6). Photoreceptor genes, such as ABCA4, STX3, and CDHR1, are highly expressed in both humans and mice (Supporting Information Fig. S6), whereas a few others, such as STX1A, showed reduced expression in CRX+ human and mouse photoreceptors. Along these lines, KCNV2 could be a good cell surface marker for human photoreceptors, as suggested for mouse photoreceptors [57]. Interestingly, in contrast to relatively stable expression in mouse photoreceptors, we discovered higher expression of SLC6A17, SLC40A1, and KCNH2 with maturation of human photoreceptors. RTN4RL1, ST3GAL5, GNGT2, and EPHA10 could also be used as cell surface molecules to identify human cones. Several proteins, including GABRR2 and CNGB1, which are highly expressed in mouse rods but not in *Nrl*^{-/-} cones, are potential markers to identify human rod photoreceptors (Supporting Information Fig. S6).

CRX Target Gene Analysis

As CRX regulates the expression of both cone- and rod-specific genes and transcriptional targets of CRX are involved

in photoreceptor morphogenesis and function [10, 11, 58], we examined the profile of CRX target genes in GFP+ developing human photoreceptors. High confidence targets (ranked score ≥ 1.5) of CRX were inferred by integrating differentially expressed genes identified from RNA-Seq data of mouse *Crx*^{-/-} retina [33] with the CRX ChIP-seq dataset [11]. Of 111 CRX targets identified, the expression of 68 genes was detectable as early as day 37 in GFP+ photoreceptors, and a total of 83 genes were expressed by day 90 (Fig. 7). Interestingly, 28 CRX target genes (highlighted with blue border nodes) that were undetectable in developing human photoreceptors include several key proteins, such as ESRRB and MEF2C which modulate the expression of many photoreceptor genes [52, 59], and FSCN2, RDH8, and RHO that are critical for photoreceptor morphogenesis and function. Ingenuity pathway analysis of CRX target genes highlighted the pathways associated with photoreceptor development and disease (data not shown). As predicted, several of the CRX targets that are not expressed until day 90 (Fig. 7) in human photoreceptors (equivalent to Fwk 13) belonged to pathways involved in organogenesis and phototransduction.

DISCUSSION

The design of stem cell-based therapies for retinal and macular degenerative diseases requires a fundamental understanding of human photoreceptor development, and identification of surface markers is critical for isolating cells at defined stages. Our current knowledge of molecules and pathways associated with rod or cone differentiation is largely based on studies in model organisms, including rodents. The recently developed PSC cell-derived 3D retina cultures provide an efficient in vitro model to delineate the biology of human photoreceptors and illustrate other developmental events. To elucidate human rod and cone development, we introduced a CRXp-GFP reporter construct into the AAVS1 locus of a well-characterized H9 hESC parental line. We show that the reporter construct recapitulates endogenous CRX expression at all stages of development examined in our in vitro 3D culture system. Human ESC-derived retinal precursor cells express panels of photoreceptor proteins at an appropriate stage of development, and the cultures can be maintained for a time period sufficient to assess early development events in the neural retina. Using this system, we have identified a window for cone and early rod precursor differentiation and with GFP fluorescence as a surrogate we were able to purify sufficient numbers of cells to collect transcriptome datasets that correlate with stages of photoreceptor development. Cellular and molecular details of human photoreceptors support hESC-3D culture [25] as a useful in vitro model system to advance our understanding of human eye development. A detailed transcriptome analysis of developing human photoreceptors provides opportunities to study fundamental biological questions and should assist in designing cell-based therapy.

A major challenge in creating a model system is the ability to recapitulate phenotypes during human development and pathogenesis. Transcript analysis of human fetal retina has been limited to a few photoreceptor genes in samples with age limit (>9 weeks postconception [p.c.]) [17, 60]. Expression of these genes (such as CRX at ~ week 6) in GFP+

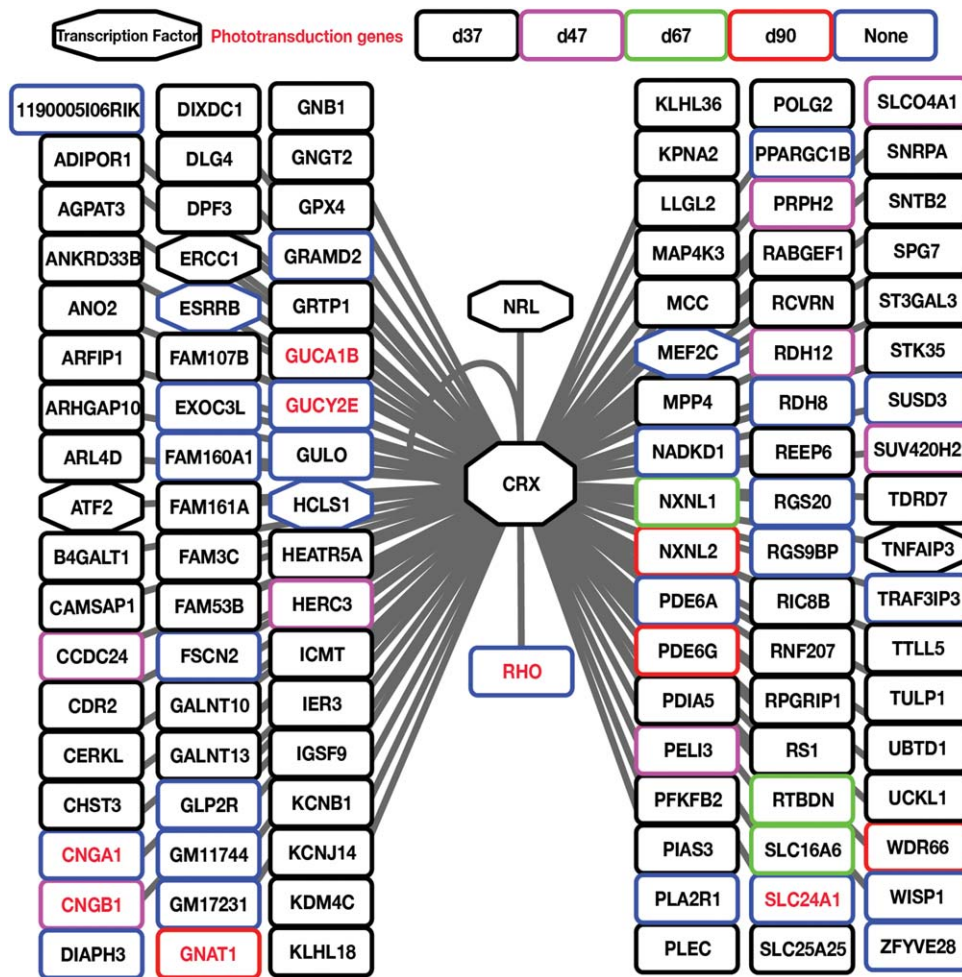


Figure 7. CRX target networks. Genes are listed with color border nodes indicating the expression at different 3D retina stages. CRX target genes with blue border nodes are undetectable in GFP+ photoreceptors (<1 FPKM). Abbreviation: CRX, cone-rod homeobox.

photoreceptors occurs before that has been detected in human fetal retina (CRX at ~10 weeks p.c.) [17, 60]. This does not necessarily mean that development of photoreceptors in 3D retina is faster compared to that observed in vivo. Our transcriptome is generated from purified developing photoreceptors, and therefore photoreceptor-associated transcripts are enriched when compared with whole retina. In addition, the temporal expression sequence of CRX, NRL, and NR2E3 in human fetal retina is replicated in 3D retina [17, 60]. Therefore, 3D retina generated from stem cells by us and by others [25, 28, 31, 61] seems to represent early stages of fetal retinal development and GFP+ photoreceptors recapitulate the differentiation sequence in vivo.

3D retina cultures have the potential to provide unique new insights into human retinal development. For example, the fovea is pure cone only region in the center of the retina, and this structural specification is not present in mouse retina. Moreover, the time frame of cone and rod differentiation is rather short during mouse retinal development since at embryonic days 13–18 both cones and rods are specified [6]. It appears that the first cells to express CRX in developing human retina and 3D retina are new-born cone photoreceptors as early expression of CRX coincides with cone birth, which occurs before rod genesis [16, 62]. A significant obser-

vation from our studies is the concurrent expression of retina and anterior neural fold homeobox 2 (RAX2) transcription factor with CRX in 3D retina. RAX2 is not present in the rodent evolutionary lineage [63], and therefore its in vivo function remains uncharacterized. RAX2 reportedly transactivates Ret-1 element for rhodopsin expression in the presence of CRX and NRL [64], and RAX2 ortholog in chicken is suggested to regulate cone genesis [65]. Thus, RAX2 may participate in cone development in human retina as its expression precedes NRL and NR2E3.

Some of the molecules expressed in human and mouse retina may have different molecular control mechanisms. For example, *PDE6B* is a target of NRL and encodes rod-specific beta subunit of cGMP phosphodiesterase, whose expression follows NRL in rodents [66–68]. In contrast, *PDE6B* mRNA is detected earlier than NRL in developing human retina [17, 60]; this observation is concordant with our gene profiling of photoreceptors from 3D retina. These studies indicate temporal and spatial differences between species [69], which might explain, in part, the failure to fully reproduce the human condition in mouse models.

3D neural retina derived from pluripotent stem cells has potential application for investigating functions of retina-expressed genes. CRX controls the expression of multiple

components of phototransduction cascade as well as specialized structural proteins involved in photoreceptor morphogenesis [10, 11, 58]. Investigation of CRX targets identified from mouse datasets in the human photoreceptor transcriptome data has revealed new insights in conserved molecules required for functional maturation, which does not occur in stem cell-derived photoreceptors by day 90. Our studies thus provide an opportunity to introduce exogenous factors that are not detected in human CRX target network for evaluating their cognate functions in 3D retina at defined stages. For example, transcription factors known to promote rhodopsin expression, ESRRB and MEF2C, are not expressed in 3D retina at day 90. These factors are also not detected in *Nrl*^{-/-} mice [52, 53] indicating that NRL is upstream regulator of ESRRB and MEF2C. Interestingly, rhodopsin immunostaining was localized in a subpopulation of GFP+/CRX+ cells at day 150, but by day 180 most GFP+ cells expressed M/L or S opsin and not rhodopsin (Supporting Information Fig. S2B, S2C). It is likely that CRX functions to initiate rhodopsin expression in human photoreceptors but is not required to maintain rhodopsin transcription at least in our 3D culture conditions. In mature rods, multiple regulatory proteins are crucial to maintain rhodopsin expression; it will therefore be interesting to investigate whether forced expression of ESRRB and MEF2C will accelerate or maintain rhodopsin expression in 3D retina. Furthermore, hematopoietic cell-specific Lyn substrate 1 (HCLS1) mediates multiple signaling events leading to transcription activation and actin remodeling in immune cells [70]. Whether CRX-target HCLS1 isoform has a role in photoreceptor morphogenesis remains to be elucidated.

Fetal-like cells generated from pluripotent stem cells have been successfully used to model early-onset neuronal diseases, such as familial dysautonomia [71]. At this stage, functionality and phenotype of the adult retina cannot be reproduced in 3D cultures, in part because of the lack of outer segments and appropriate synaptic connectivity of photoreceptors; thus, 3D retina is currently not appropriate for modeling late-onset retinal degenerative diseases.

The feasibility of photoreceptor replacement has been demonstrated in mouse models [55] where committed yet immature rod photoreceptors that express *Nrl* [56] can integrate into degenerating retina and restore some visual function [55, 72, 73]. No data on the feasibility of this approach are available in humans, but our system would permit such investigations. A photoreceptor stage may also contribute to cone or rod subtypes upon transplantation [74] and should be considered when designing treatment of cone or rod degeneration. The gene profiles and cell surface molecules, reported here, require further validation; nonetheless, our studies serve

as a starting point for isolating human photoreceptors at specific stage(s) of differentiation and for their use in cell replacement therapy.

CONCLUSIONS

We have defined molecular signatures associated with the development of human photoreceptors using hESC-derived 3D retina as an in vitro model system. The 3D cultures appear to recapitulate the time course of retinal differentiation in vivo, while concurrently demonstrating commonalities and distinctions between humans and mice. Molecular signatures, reported here, provide the foundation for defining pathways underlying human photoreceptor development and consequently help in the design of treatment paradigms for retinal degenerative diseases.

ACKNOWLEDGMENTS

This research was supported by Intramural Research Program (Z01 EY000450 and EY000474) of the National Eye Institute, National Institutes of Health. K.H. was supported by grant-in-aid for Young Scientists (B) from Japan Society for the Promotion of Science (JSPS) and JSPS Postdoctoral Fellowships for Research Abroad (Kaitoku-NIH). We thank Linn Gieser, Rafael Villasmil, Trevor Cerbini, and Jacklyn Mahgerefteh for technical assistance, Robert Fariss and Chun Gao for assistance with live imaging, and Tiziana Coglaiti for helpful comments and discussion. K.H. is currently affiliated with Department of Physiology, Nippon Medical School, Tokyo, Japan. M.R. is currently affiliated with The New York Stem Cell Foundation Research Institute, New York, NY.

AUTHOR CONTRIBUTIONS

R.K.: conception and design, collection and/or assembly of data, data analysis and interpretation, manuscript writing, and approved the final manuscript; K.D.K., M.B., and V.C.: data analysis and interpretation and approved the final manuscript; K.H. and J.Z.: provision of study material and approved the final manuscript; M.R.: provision of study material, manuscript writing, and approved the final manuscript; A.S.: conception and design, data analysis and interpretation, financial support, administrative support, manuscript writing, and approved the final manuscript.

DISCLOSURE OF POTENTIAL CONFLICTS OF INTEREST

The authors indicate no potential conflicts of interest.

REFERENCES

- Curcio CA, Sloan KR, Kalina RE et al. Human photoreceptor topography. *J Comp Neurol* 1990;292:497–523.
- Provis JM, Diaz CM, Dreher B. Ontogeny of the primate fovea: A central issue in retinal development. *Prog Neurobiol* 1998;54:549–580.
- Curcio CA. Photoreceptor topography in ageing and age-related maculopathy. *Eye (Lond)* 2001;15:376–383.
- Wright AF, Chakarova CF, Abd El-Aziz MM et al. Photoreceptor degeneration: Genetic and mechanistic dissection of a complex trait. *Nat Rev Genet* 2010;11:273–284.
- Allison WT, Barthel LK, Skebo KM et al. Ontogeny of cone photoreceptor mosaics in zebrafish. *J Comp Neurol* 2010;518:4182–4195.
- Swaroop A, Kim D, Forrest D. Transcriptional regulation of photoreceptor development and homeostasis in the mammalian retina. *Nat Rev Neurosci* 2010;11:563–576.
- Agathocleous M, Harris WA. From progenitors to differentiated cells in the vertebrate retina. *Annu Rev Cell Dev Biol* 2009;25:45–69.

- 8 Sanes JR, Zipursky SL. Design principles of insect and vertebrate visual systems. *Neuron* 2010;66:15–36.
- 9 Muranishi Y, Sato S, Inoue T et al. Gene expression analysis of embryonic photoreceptor precursor cells using BAC-Crx-EGFP transgenic mouse. *Biochem Biophys Res Commun* 2010;392:317–322.
- 10 Furukawa T, Morrow EM, Li T et al. Retinopathy and attenuated circadian entrainment in Crx-deficient mice. *Nat Genet* 1999;23:466–470.
- 11 Corbo JC, Lawrence KA, Karlstetter M et al. CRX ChIP-seq reveals the cis-regulatory architecture of mouse photoreceptors. *Genome Res* 2010;20:1512–1525.
- 12 Mears AJ, Kondo M, Swain PK et al. Nrl is required for rod photoreceptor development. *Nat Genet* 2001;29:447–452.
- 13 Ng L, Hurley JB, Dierks B et al. A thyroid hormone receptor that is required for the development of green cone photoreceptors. *Nat Genet* 2001;27:94–98.
- 14 Oh EC, Khan N, Novelli E et al. Transformation of cone precursors to functional rod photoreceptors by bZIP transcription factor NRL. *Proc Natl Acad Sci USA* 2007;104:1679–1684.
- 15 Ng L, Lu A, Swaroop A et al. Two transcription factors can direct three photoreceptor outcomes from rod precursor cells in mouse retinal development. *J Neurosci* 2011;31:11118–11125.
- 16 Hendrickson A, Bumsted-O'Brien K, Natoli R et al. Rod photoreceptor differentiation in fetal and infant human retina. *Exp Eye Res* 2008;87:415–426.
- 17 Bumsted O'Brien Keely KM, Schulte D, Hendrickson AE. Expression of photoreceptor-associated molecules during human fetal eye development. *Mol Vis* 2003;9:401–409.
- 18 Takahashi K, Tanabe K, Ohnuki M et al. Induction of pluripotent stem cells from adult human fibroblasts by defined factors. *Cell* 2007;131:861–872.
- 19 Thomson JA, Itskovitz-Eldor J, Shapiro SS et al. Embryonic stem cell lines derived from human blastocysts. *Science* 1998;282:1145–1147.
- 20 Pera MF, Trounson AO. Human embryonic stem cells: Prospects for development. *Development* 2004;131:5515–5525.
- 21 Boucherie C, Mukherjee S, Henckaerts E et al. Brief report: Self-organizing neuroepithelium from human pluripotent stem cells facilitates derivation of photoreceptors. *Stem Cells* 2013;31:408–414.
- 22 Meyer JS, Shearer RL, Capowski EE et al. Modeling early retinal development with human embryonic and induced pluripotent stem cells. *Proc Natl Acad Sci USA* 2009;106:16698–16703.
- 23 Osakada F, Ikeda H, Mandai M et al. Toward the generation of rod and cone photoreceptors from mouse, monkey and human embryonic stem cells. *Nat Biotechnol* 2008;26:215–224.
- 24 Lamba DA, Karl MO, Reh TA. Strategies for retinal repair: Cell replacement and regeneration. *Prog Brain Res* 2009;175:23–31.
- 25 Nakano T, Ando S, Takata N et al. Self-formation of optic cups and storable stratified neural retina from human ESCs. *Cell Stem Cell* 2012;10:771–785.
- 26 Zhong X, Gutierrez C, Xue T et al. Generation of three-dimensional retinal tissue with functional photoreceptors from human iPSCs. *Nat Commun* 2014;5:4047.
- 27 Meyer JS, Howden SE, Wallace KA et al. Optic vesicle-like structures derived from human pluripotent stem cells facilitate a customized approach to retinal disease treatment. *Stem Cells* 2011;29:1206–1218.
- 28 Reichman S, Terray A, Slembrouck A et al. From confluent human iPSCs to self-forming neural retina and retinal pigmented epithelium. *Proc Natl Acad Sci USA* 2014;111:8518–8523.
- 29 Furukawa A, Koike C, Lippincott P et al. The mouse Crx 5'-upstream transgene sequence directs cell-specific and developmentally regulated expression in retinal photoreceptor cells. *J Neurosci* 2002;22:1640–1647.
- 30 Matsuda T, Cepko CL. Analysis of gene function in the retina. *Methods Mol Biol* 2008;423:259–278.
- 31 Mellough CB, Collin J, Khazim M et al. IGF-1 signaling plays an important role in the formation of three-dimensional laminated neural retina and other ocular structures from human embryonic stem cells. *Stem Cells* 2015;33:2416–2430.
- 32 Kuwahara A, Ozone C, Nakano T et al. Generation of a ciliary margin-like stem cell niche from self-organizing human retinal tissue. *Nat Commun* 2015;6:6286.
- 33 Roger JE, Hiriyanna A, Gotoh N et al. OTX2 loss causes rod differentiation defect in CRX-associated congenital blindness. *J Clin Invest* 2014;124:631–643.
- 34 Brooks MJ, Rajasimha HK, Swaroop A. Retinal transcriptome profiling by directional next-generation sequencing using 100 ng of total RNA. *Methods Mol Biol* 2012;884:319–334.
- 35 Brooks MJ, Rajasimha HK, Roger JE et al. Next-generation sequencing facilitates quantitative analysis of wild-type and Nrl(-/-) retinal transcriptomes. *Mol Vis* 2011;17:3034–3054.
- 36 Young RW. Cell proliferation during postnatal development of the retina in the mouse. *Brain Res* 1985;353:229–239.
- 37 Young RW. Cell differentiation in the retina of the mouse. *Anat Rec* 1985;212:199–205.
- 38 Hsieh Y-W, Yang X-J. Dynamic Pax6 expression during the neurogenic cell cycle influences proliferation and cell fate choices of retinal progenitors. *Neural Dev* 2009;4:32.
- 39 Oron-Karni V, Farhy C, Elgart M et al. Dual requirement for Pax6 in retinal progenitor cells. *Development* 2008;135:4037–4047.
- 40 Zhu CC, Dyer MA, Uchikawa M et al. Six3-mediated auto repression and eye development requires its interaction with members of the Groucho-related family of co-repressors. *Development* 2002;129:2835–2849.
- 41 Nishida A, Furukawa A, Koike C et al. Otx2 homeobox gene controls retinal photoreceptor cell fate and pineal gland development. *Nat Neurosci* 2003;6:1255–1263.
- 42 Brzezinski JAT, Uoon Park K, Reh TA. Blimp1 (Prdm1) prevents re-specification of photoreceptors into retinal bipolar cells by restricting competence. *Dev Biol* 2013;384:194–204.
- 43 Kautzmann MA, Kim DS, Felder-Schmittbuhl MP et al. Combinatorial regulation of photoreceptor differentiation factor, neural retina leucine zipper gene NRL, revealed by in vivo promoter analysis. *J Biol Chem* 2011;286:28247–28255.
- 44 Montana CL, Lawrence KA, Williams NL et al. Transcriptional regulation of neural retina leucine zipper (Nrl), a photoreceptor cell fate determinant. *J Biol Chem* 2011;286:36921–36931.
- 45 Oh EC, Cheng H, Hao H et al. Rod differentiation factor NRL activates the expression of nuclear receptor NR2E3 to suppress the development of cone photoreceptors. *Brain Res* 2008;1236:16–29.
- 46 Fujitani Y, Fujitani S, Luo H et al. Ptf1a determines horizontal and amacrine cell fates during mouse retinal development. *Development* 2006;133:4439–4450.
- 47 Wu F, Li R, Umino Y et al. Onecut1 is essential for horizontal cell genesis and retinal integrity. *J Neurosci* 2013;33:13053–13065.
- 48 Li S, Mo Z, Yang X et al. Foxn4 controls the genesis of amacrine and horizontal cells by retinal progenitors. *Neuron* 2004;43:795–807.
- 49 Mu X, Fu X, Beremand PD et al. Gene regulation logic in retinal ganglion cell development: Isl1 defines a critical branch distinct from but overlapping with Pou4f2. *Proc Natl Acad Sci USA* 2008;105:6942–6947.
- 50 Nelson BR, Ueki Y, Reardon S et al. Genome-wide analysis of Müller glial differentiation reveals a requirement for notch signaling in postmitotic cells to maintain the glial fate. *PLoS One* 2011;6:e22817.
- 51 Roesch K, Jadhav AP, Trimarchi JM et al. The transcriptome of retinal Müller glial cells. *J Comp Neurol* 2008;509:225–238.
- 52 Hao H, Tummala P, Guzman E et al. The transcription factor neural retina leucine zipper (NRL) controls photoreceptor-specific expression of myocyte enhancer factor Mef2c from an alternative promoter. *J Biol Chem* 2011;286:34893–34902.
- 53 Onishi A, Peng G-H, Poth EM et al. The orphan nuclear hormone receptor ERR β controls rod photoreceptor survival. *Proc Natl Acad Sci USA* 2010;107:11579–11584.
- 54 Ng L, Hurley JB, Dierks B et al. A thyroid hormone receptor that is required for the development of green cone photoreceptors. *Nat Genet* 2001;27:94–98.
- 55 MacLaren RE, Pearson RA, MacNeil A et al. Retinal repair by transplantation of photoreceptor precursors. *Nature* 2006;444:203–207.
- 56 Akimoto M, Cheng H, Zhu D et al. Targeting of GFP to newborn rods by Nrl promoter and temporal expression profiling of flow-sorted photoreceptors. *Proc Natl Acad Sci USA* 2006;103:3890–3895.
- 57 Postel K, Bellmann J, Splith V et al. Analysis of cell surface markers specific for transplantable rod photoreceptors. *Mol Vis* 2013;19:2058–2067.
- 58 Hennig AK, Peng GH, Chen S. Regulation of photoreceptor gene expression by Crx

associated transcription factor network. *Brain Res* 2008;1192:114–133.

59 Onishi A, Peng GH, Poth EM et al. The orphan nuclear hormone receptor ERRbeta controls rod photoreceptor survival. *Proc Natl Acad Sci USA* 2010;107:11579–11584.

60 Bibb LC, Holt JK, Tarttelin EE et al. Temporal and spatial expression patterns of the CRX transcription factor and its downstream targets. Critical differences during human and mouse eye development. *Hum Mol Genet* 2001;10:1571–1579.

61 Zhong X, Gutierrez C, Xue T et al. Generation of three-dimensional retinal tissue with functional photoreceptors from human iPSCs. *Nat Commun* 2014;5:4047.

62 Xiao M, Hendrickson A. Spatial and temporal expression of short, long/medium, or both opsins in human fetal cones. *J Comp Neurol* 2000;425:545–559.

63 Zhong Y-F, Holland P. The dynamics of vertebrate homeobox gene evolution: Gain and loss of genes in mouse and human lineages. *BMC Evol Biol* 2011;11:169.

64 Wang QL, Chen S, Esumi N et al. QRX, a novel homeobox gene, modulates photoreceptor gene expression. *Hum Mol Genet* 2004;13:1025–1040.

65 Chen C-MA, Cepko CL. The chicken RaxL gene plays a role in the initiation of photoreceptor differentiation. *Development* 2002;129:5363–5375.

66 Hao H, Kim DS, Klocke B et al. Transcriptional regulation of rod photoreceptor homeostasis revealed by in vivo NRL targetome analysis. *PLoS Genet* 2012;8:e1002649.

67 Yoshida S, Mears AJ, Friedman JS et al. Expression profiling of the developing and mature Nrl^{-/-} mouse retina: Identification of retinal disease candidates and transcriptional regulatory targets of Nrl. *Hum Mol Genet* 2004;13:1487–1503.

68 He L CM, Srivastava D, Blocker YS, Harris JR, Swaroop A, Fox DA. Spatial and temporal expression of AP-1 responsive rod photoreceptor genes and bZIP transcription factors during development of the rat retina. *Mol Vis* 1998;4:32.

69 Fougerousse F, Bullen P, Herasse M et al. Human–mouse differences in the

embryonic expression patterns of developmental control genes and disease genes. *Hum Mol Genet* 2000;9:165–173.

70 Gomez TS, McCarney SD, Carrizosa E et al. HS1 functions as an essential actin-regulatory adaptor protein at the immune synapse. *Immunity* 2006;24:741–752.

71 Lee G, Studer L. Modelling familial dysautonomia in human induced pluripotent stem cells. *Philos Trans R Soc Lond B Biol Sci* 2011;366:2286–2296.

72 Barber AC, Hippert C, Duran Y et al. Repair of the degenerate retina by photoreceptor transplantation. *Proc Natl Acad Sci USA* 2013;110:354–359.

73 Pearson RA, Barber AC, Rizzi M et al. Restoration of vision after transplantation of photoreceptors. *Nature* 2012;485:99–103.

74 Lakowski J, Baron M, Bainbridge J et al. Cone and rod photoreceptor transplantation in models of the childhood retinopathy Leber congenital amaurosis using flow-sorted Crx-positive donor cells. *Hum Mol Genet* 2010;19:4545–4559.



See www.StemCells.com for supporting information available online.